

Exploring the Impact of Image Resolution on Chest X-ray Classification Performance

Alessandro Wollek¹, Sardi Hyska², Bastian Sabel², Michael Ingrischi²,
Tobias Lasser¹

¹Munich Institute of Biomedical Engineering and the School of Computation, Information, and Technology, Technical University of Munich

²Department of Radiology, University Hospital Ludwig-Maximilians-Universität

Corresponding author: Alessandro Wollek, email: alessandro.wollek@tum.de, address: Boltzmannstr. 11, 85748 Garching, Germany

Abstract

Deep learning models for image classification have often used a resolution of 224×224 pixels for computational reasons. This study investigates the effect of image resolution on chest X-ray classification performance, using the ChestX-ray14 dataset. The results show that a higher image resolution, specifically 1024×1024 pixels, has the best overall classification performance, with a slight decline in performance between 256×256 to 512×512 pixels for most of the pathological classes. Comparison of saliency map-generated bounding boxes revealed that commonly used resolutions are insufficient for finding most pathologies.

1. Introduction

Since AlexNet, images processed by deep learning models are often resized to 224×224 pixels during training^{1,2,3,4}, mostly for computational reasons. Training at a lower resolution requires less memory and consequently models train faster. Tan and Le studied the importance of image resolution on image classification accuracy on ImageNet⁴. Valuing image resolution as a parameter similar to network depth or width. For chest radiographs, Sabottke and Spieler tested different image resolutions (32×32 up to 600×600 pixels) for chest X-ray classification⁵. In their experiments, maximum classification AUCs were obtained between 256×256 and 448×448 pixels resolution. Chest radiographs, on the other hand, have often a resolution of 2500×3500 pixels. While the images of the chest X-ray 14 data set⁶ were down-scaled to 1024×1024 pixels, it is the only large publicly available data set that also contains bounding boxes for eight pathologies. In this study, we investigate the effect of image resolution on chest X-ray classification performance.

Effect of Image Resolution on Saliency Map

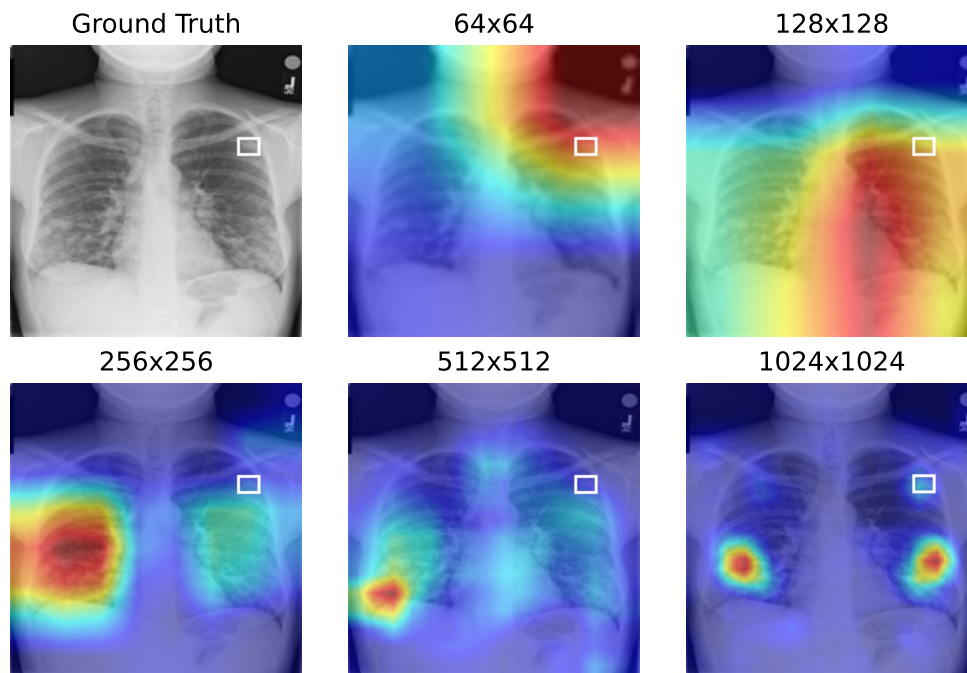


Figure 1: GradCAM saliency maps for different image resolutions. The annotated nodule bounding box is overlaid in white.

II. Methods

Subsequent models were trained on the chest X-ray 14 data set containing 112,120 frontal view chest radiographs from 32717 patients⁶. The test data set, contains a small sub set (983 images) with bounding box annotations for the eight findings: atelectasis, effusion, mass, cardiomegaly, infiltration, pneumonia, nodule, and pneumothorax. We used the development/test split provided by the authors and split the development split into Before model training, images were resized to 64×64 , 128×128 , 256×256 , 512×512 , and the full 1024×1024 pixel resolution.

II.A. Chest X-ray Classification

For classification, a DenseNet-121² pre-trained on the ImageNet⁷ data set was used. To predict the 14 chest X-ray 14 classes, we replaced the last fully-connected layer with one with 14 output dimensions. We trained the model with binary cross entropy loss and used AdamW⁸ for optimization.

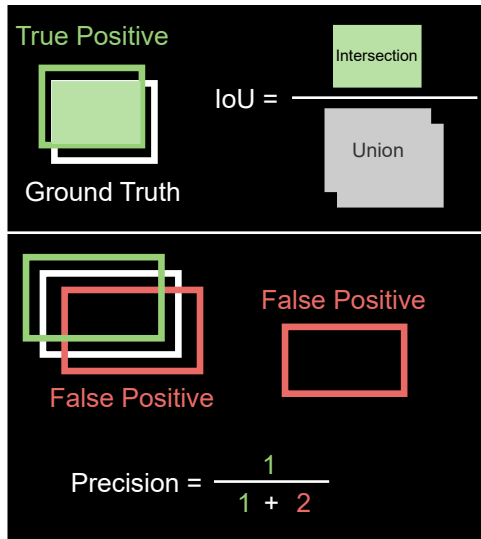


Figure 2: Evaluation of saliency map localization with precision at specific intersection over union. A prediction must overlap sufficiently, determined by the intersection over union (IoU) threshold. Only a single overlapping detection is considered a true positive. The precision is the number of true positives divided by the number of detections.

II.B. Object Detection

Given the bounding box annotations for eight of the 14 findings, we investigated the effect of image resolution on predicted bounding boxes. We created binary segmentations from GradCAM⁹ saliency maps generated by the penultimate layer by first normalizing them and then applying a threshold of 0.5. To create bounding boxes, we extracted the connected components and calculated the surrounding bounding boxes.

For each predicted, and annotated bounding box we calculated the intersection over union (IoU)

$$\text{IoU}(A, B) = \frac{A \cap B}{A \cup B},$$

shown in Figure 2, and the class-wise mean precision. The precision is defined as the number of true positives divided by the number of detections¹. Since the chest X-ray 14 data set contains only one segmentation per sample, the precision is either 0 or 1 over the number of detections. A detection was considered positive, if the IoU was at least 0.1 ($\text{IoU} \geq 0.1$). Out of multiple sufficiently overlapping detection only one was considered as a true positive.

Finding	64×64	128×128	256×256	512×512	1024×1024
Atelectasis	0.760	0.800	0.810	0.807	0.821
Cardiomegaly	0.858	0.900	0.906	0.909	0.908
Consolidation	0.752	0.787	0.797	0.794	0.797
Edema	0.866	0.869	0.885	0.878	0.891
Effusion	0.845	0.873	0.877	0.874	0.879
Emphysema	0.824	0.884	0.900	0.913	0.937
Fibrosis	0.748	0.803	0.816	0.821	0.850
Hernia	0.865	0.926	0.903	0.895	0.916
Infiltration	0.678	0.707	0.714	0.699	0.714
Mass	0.765	0.827	0.830	0.813	0.829
Nodule	0.669	0.719	0.761	0.780	0.803
Pleural Thickening	0.730	0.751	0.757	0.763	0.796
Pneumonia	0.688	0.743	0.760	0.760	0.769
Pneumothorax	0.799	0.839	0.858	0.859	0.877
Mean	0.775	0.816	0.827	0.826	0.842

Table 1: Chest X-ray classification AUCs for different image resolutions. Highest values are highlighted in bold.

III. Results

III.A. Chest X-ray Classification

Per-class AUC scores are provided in table 1. Unsurprisingly, the model trained on only 64×64 pixel images scored the lowest, with a mean AUC of 77.5 %. The highest resolution, 1024×1024 pixels, performed best with a mean AUC of 84.2 %, followed by 256×256 pixels with a mean AUC of 82.7 %.

III.B. Object Detection

When increasing image resolution, the generated GradCAM saliency maps became more detailed due to the larger output size before the global average pooling layer. An example is shown in Figure 1.

Mean precision @ IoU ≥ 0.1 results are shown in Table 2. For most classes, the highest resolution, 1024×1024 pixels, had the highest precision, except for cardiomegaly, infiltration, and pneumothorax. Where 256×256 (cardiomegaly, pneumothorax) and 128×128 (infiltration) performed best.

The mean precision @ IoU ≥ 0.1 show that, although the saliency maps were smaller they were more precise. Ignoring the number of false positives, i.e., how many saliency map-based

¹For a more general explanation of object detection metrics, such as IoU and average precision we refer to¹⁰.

Finding	64×64	128×128	256×256	512×512	1024×1024
Atelectasis	0.001	0.117	0.120	0.361	0.395
Effusion	0.004	0.036	0.310	0.353	0.356
Mass	0.004	0.003	0.330	0.417	0.508
Cardiomegaly	0.114	0.804	0.946	0.792	0.242
Infiltration	0.008	0.283	0.084	0.201	0.200
Pneumonia	0.095	0.370	0.189	0.394	0.402
Nodule	0.000	0.000	0.000	0.150	0.326
Pneumothorax	0.003	0.061	0.391	0.180	0.198

Table 2: Mean precision at intersection over union ≥ 10 % of chest pathology bounding boxes and binary saliency maps.

segmentations were generated for a single ground truth and focusing on the maximum IoU per sample draws a similar pictures, as shown in Table 3. While the highest resolution, 1024×1024 , was the most precise except for cardiomegaly, infiltration, and pneumothorax, the highest average IoU was only highest for mass, nodule, and pneumothorax. For example, on average cardiomegaly bounding boxes and generated bounding boxes at 256×256 resolution had, on average, an IoU of 60.1 % compared, the highest resolution was worst with only 11.4 % IoU. We interpret these results, due to the nature of cardiomegaly bounding boxes that are the largest for this data set and that saliency maps for the highest resolution are small(er) than the annotated bounding boxes. This hypothesis is supported by the results that at lower resolutions (128 - 512) cardiomegaly mean precision was significantly higher than for the highest resolution. The findings are inverted for the smallest pathology, lung nodules. Here, the bounding boxes from the highest resolution have a significantly higher mean precision and maximum IoU than all other resolutions. While these results suggest that a lower resolution improves classification performance of larger pathologies, the test AUCs in Table 1 show that the effect on classification performance is only noticeable for the class hernia. For example, for pneumothorax the highest resolution achieved the highest mean AUC. We interpret these results, due to the kind of pathology. Signs of a pneumothorax, for example, could be only a long curve. Hence, the surrounding bounding box would cover a much larger area than the actual pathology.

Finding	64×64	128×128	256×256	512×512	1024×1024
Atelectasis	0.030	0.049	0.071	0.196	0.177
Effusion	0.053	0.057	0.158	0.209	0.168
Mass	0.034	0.066	0.124	0.216	0.340
Cardiomegaly	0.126	0.280	0.609	0.264	0.114
Infiltration	0.100	0.164	0.092	0.133	0.055
Pneumonia	0.052	0.106	0.172	0.206	0.133
Nodule	0.003	0.008	0.023	0.073	0.228
Pneumothorax	0.050	0.080	0.126	0.109	0.168

Table 3: Mean max intersection over union

IV. Discussion

In this chapter, we studied the importance of chest X-ray resolution on image classification performance. The classification results (see Table 1) suggest that overall a higher resolution improves image classification performance. The highest available resolution, 1024×1024 , performed best for all findings except cardiomegaly, hernia, and mass. For these, it performed second to best. While Sabottke and Spieler achieved maximum AUCs between 256×256 and 448×448 pixels resolution, they tested only up to 600×600 pixels. We observed a slight decline in AUC from 256×256 to 512×512 pixel resolution for most (9/14) classes. These findings are in line with the conclusion of Tan and Le that their highest tested resolution 600×600 was not optimal. However, our results show that an even higher image resolution, 1024×1024 pixels, improved chest X-ray classification performance. Similar results were shown for image classification accuracy on ImageNet⁴.

In summary, we investigated the effect of image resolution on chest X-ray classification and localization. Our results showed that a higher resolution of 1024×1024 performed best.

V. Acknowledgments

This work was supported in part by the German federal ministry of health’s program for digital innovations for the improvement of patient-centered care in healthcare [grant agreement no. 2520DAT920].

- ¹ A. Krizhevsky, I. Sutskever, and G. E. Hinton, Imagenet Classification with Deep Convolutional Neural Networks, *Advances in neural information processing systems* **25**, 1097–1105 (2012).
- ² G. Huang, Z. Liu, L. Van Der Maaten, and K. Q. Weinberger, Densely Connected Convolutional Networks, in *Proceedings of the IEEE Conference on Computer Vision and Pattern Recognition*, pages 4700–4708, 2017.
- ³ K. He, X. Zhang, S. Ren, and J. Sun, Deep Residual Learning for Image Recognition, in *Proceedings of the IEEE Conference on Computer Vision and Pattern Recognition*, pages 770–778, 2016.
- ⁴ M. Tan and Q. V. Le, EfficientNet: Rethinking Model Scaling for Convolutional Neural Networks, [arXiv:1905.11946](https://arxiv.org/abs/1905.11946) [cs, stat] (2020).
- ⁵ C. F. Sabottke and B. M. Spieler, The Effect of Image Resolution on Deep Learning in Radiography, *Radiology: Artificial Intelligence* **2**, e190015 (2020).

- ⁶ X. Wang, Y. Peng, L. Lu, Z. Lu, M. Bagheri, and R. M. Summers, ChestX-ray8: Hospital-scale Chest X-ray Database and Benchmarks on Weakly-Supervised Classification and Localization of Common Thorax Diseases, in *2017 IEEE Conference on Computer Vision and Pattern Recognition (CVPR)*, pages 3462–3471, 2017.
- ⁷ J. Deng, W. Dong, R. Socher, L.-J. Li, K. Li, and L. Fei-Fei, ImageNet: A Large-Scale Hierarchical Image Database, in *2009 IEEE Conference on Computer Vision and Pattern Recognition*, pages 248–255, 2009.
- ⁸ I. Loshchilov and F. Hutter, Decoupled Weight Decay Regularization, in *International Conference on Learning Representations*, 2018.
- ⁹ R. R. Selvaraju, M. Cogswell, A. Das, R. Vedantam, D. Parikh, and D. Batra, Grad-CAM: Visual Explanations From Deep Networks via Gradient-Based Localization, in *Proceedings of the IEEE International Conference on Computer Vision*, pages 618–626, 2017.
- ¹⁰ R. Padilla, S. L. Netto, and E. A. da Silva, A Survey on Performance Metrics for Object-Detection Algorithms, in *2020 International Conference on Systems, Signals and Image Processing (IWSSIP)*, pages 237–242, IEEE, 2020.